Carbohydrate Polymers 94 (2013) 603–611

Contents lists available at SciVerse ScienceDirect

Carbohydrate Polymers

journal homepage: www.elsevier.com/locate/carbpol

Bacterial cellulose and bacterial cellulose–chitosan membranes for wound dressing applications

Wen-Chun Lin[a], Chun-Chieh Lien[b], Hsiu-Jen Yeh[b], Chao-Ming Yu[b], Shan-hui Hsu[a,*]

[a] Institute of Polymer Science and Engineering, National Taiwan University, Taipei, Taiwan
[b] Chia Meei Food Industrial Corporation, Taichung, Taiwan

ARTICLE INFO

Article history:
Received 8 May 2012
Received in revised form 8 August 2012
Accepted 25 January 2013
Available online 1 February 2013

Keywords:
Bacterial cellulose
Chitosan
Wound dressing
Biocompatibility

ABSTRACT

Bacterial cellulose (BC) and bacterial cellulose–chitosan (BC–Ch) membranes were successfully produced in large scale. BC was synthesized by *Acetobacter xylinum*. BC–Ch was prepared by immersing BC in chitosan followed by freeze-drying. The surface morphology of BC and BC–Ch membranes were examined by a scanning electron microscope (SEM). SEM images showed that BC–Ch possessed a denser fibril network with smaller pores than BC. Infrared spectroscopy was used to confirm the incorporation of chitosan in BC–Ch. The swelling behavior, water retention capacity, and mechanical properties of BC and BC–Ch were further evaluated. Results indicated that both membranes maintained proper moisture contents for an extensive period without dehydration. The tensile strength and elongation at break for BC–Ch were slightly lower while the Young's modulus was higher. Cell culture studies demonstrated that BC and BC–Ch had no cytotoxicity. In the antibacterial test, the addition of chitosan in BC showed significant growth inhibition against *Escherichia coli* and *Staphylococcus aureus*. The effects of BC and BC–Ch on skin wound healing were assessed by rat models. Histological examinations revealed that wounds treated with BC–Ch epithelialized and regenerated faster than those treated with BC or Tegaderm. Therefore, BC–Ch was considered as a potential candidate for wound dressing materials.

1. Introduction

Cellulose is the most abundant organic compound in nature. Although frequently derived from plants, cellulose is also synthesized by a variety of microorganisms such as bacteria, algae and fungi. The biosynthetic bacterial cellulose (BC) is a nearly purified form of cellulose produced by strains of the Gram-negative bacterium *Acetobacter xylinum* using glucoses as the common substrate (Czaja, Krystynowicz, Bielecki, & Brown, 2006; Kurosumi, Sasaki, Yamashita, & Nakamura, 2009). BC exhibits high purity and comprises no other substances including lignin, pectin and hemicellulose while plant-derived cellulose does (Cai, Hou, & Yang, 2012). Although BC and plant cellulose possess similar chemical structure, the self-assembling nanofibrous structure of BC is different from that of plant cellulose. With the ultra-fine network structure, BC displays unique physico-chemical properties such as high tensile strength, crystallinity, and water absorption capacity (Eichhorn et al., 2001; Keshk & Sameshima, 2006; Klemm, Schumann, Udhardt, & Marsch, 2001).

The superior characteristics of BC have made it used in a number of diverse applications such as tires, paper, textiles, high quality speaker diaphragms (Nishi et al., 1990), separation membranes (Takai, 1994), and electronic paper (Shah & Brown, 2005). BC has also received considerable attention in biomedical fields because of the good biocompatibility. For instance, BC may be used in manufacturing artificial blood vessels for microsurgery (Klemm et al., 2001), scaffolds for tissue engineering (Bäckdahl et al., 2006), and wound dressings for burn or wound repair (Alvarez, Patel, Booker, & Markowitz, 2004; Legeza et al., 2004). BC shows great stability, low toxicity, non-allergenicity, and can be safely sterilized. BC, however, does not possess antibacterial ability to prevent wound infection when used in wound treatment. A few recent efforts have been made to improve the antibacterial properties of BC membranes (Cai, Hou, & Yang, 2011; Maneerung, Tokura, & Rujiravanit, 2008; Phisalaphong & Jatupaiboon, 2008).

Chitosan is a polysaccharide obtained from the N-deacetylation of chitin, consisting of polymeric (1→4)-linked 2-amino-2-deoxy-β-D-glucopyranose units (Li et al., 2007). Because of the biocompatibility, non-toxicity, biodegradability, and intrinsic antibacterial properties (Pillai, Paul, & Sharma, 2009; Rinaudo, 2006), chitosan is considered as a versatile material with potential biomedical applications. Previous studies showed that chitosan displayed a broad antibacterial spectrum against the growth of bacteria, yeast and fungi (Rabea, Badawy, Stevens, Smagghe, &

* Corresponding author at: Institute of Polymer Science and Engineering, National Taiwan University, No. 1, Sec. 4, Roosevelt Road, Taipei 10617, Taiwan. Tel.: +886 2 33665313; fax: +886 2 33665237.
E-mail address: shhsu@ntu.edu.tw (S.-h. Hsu).

0144-8617/$ – see front matter © 2013 Elsevier Ltd. All rights reserved.
http://dx.doi.org/10.1016/j.carbpol.2013.01.076

Steurbaut, 2003). Furthermore, chitosan was found to promote wound healing by accelerating the infiltration of inflammatory cells, enhancing the migration and proliferation of fibroblasts, and stimulating the production of type III collagen in the wound area (Ueno et al., 1999). These advantages make chitosan a good candidate for wound dressing applications.

In this study, BC membranes were mass-produced from *A. xylinum*. BC–Ch membranes were prepared by treating BC membranes with chitosan solution. The swelling characteristics, water retention properties, water vapor transmission, and tensile strength of BC and BC–Ch membranes were evaluated. Cytocompatibility and antibacterial activities were assessed in vitro. The effects of BC and BC–Ch on wound healing were examined in rat skin models. The composite BC–Ch membranes were developed in the hope of accelerating the wound healing process as well as decreasing the infection rate.

2. Materials and methods

2.1. Preparation of BC membranes and the BC–Ch composites

A. xylinum BCRC 14182 (purchased from the Bioresource Collection and Research Center, Hsinchu, Taiwan) was used as the acetic acid bacterial strain for the mass-production of BC (Yu & Lien, 2012). The culture medium was prepared with coconut-water and followed by addition of sugar as the carbon-source and acetic acid as the acidifier. After sterilization, the medium was inoculated with *A. xylinum* (5–10%, v/v) and cultivated statically for 3–7 days. The celluloses were collected and rinsed with deionized water several times in order to remove bacteria and nutrients. The wet BC membranes with 3–7 mm thickness, 400 mm length, and 250 mm width were then sterilized by an autoclave, and compressed to remove excess water by a compressor. Finally, the membranes were freeze-dried and used in this study. The dry BC membranes were stored at room temperature and their final thickness was 0.1–0.15 mm. To prepare BC–Ch composite membranes, chitosan was dissolved in 1% citric acid aqueous solution so the concentration of chitosan in the solution was 0.6%. Wet BC membranes were then immersed in the chitosan solution for 12 h. The end product was freeze-dried and abbreviated as BC–Ch. Chitosan used in the study was obtained from Charming & Beauty Co., Ltd. (Taiwan) with a molecular weight 30 kDa and degree of deacetylation 90%.

2.2. Characterization of BC and the composites

BC and BC–Ch membranes were characterized for surface morphology, Fourier transform infrared spectroscopy (FTIR), swelling properties, water retention, water vapor transmission and mechanical properties as described below.

2.2.1. SEM studies

The surface morphology of BC and BC–Ch was examined by scanning electron microscope (SEM, JEOL JSM-7600F, Japan). Prior to SEM observation, the membranes were lyophilized and coated with an ultrathin layer of gold in an ion sputter.

2.2.2. FTIR studies

The chemical structure of BC and BC–Ch membranes was analyzed by FTIR (PerkinElmer Spectrum 100 FTIR Spectrometer, USA) with an attenuated total reflectance (ATR) accessory. A zinc selenide (ZnSe) crystal was used for internal reflection. All membranes were lyophilized prior to FTIR measurements. Data were collected over 16 scans at 0.5 cm^{-1} resolution and analyzed using the Spectrum 10™ software.

2.2.3. Water absorptivity

The water absorptivity of membranes was determined by a gravimetric method (Li et al., 2011). Initially, membranes were cut into 4 cm × 4 cm pieces and their dry weights (W_{dry}) were accurately measured. Each sample was immersed in a vial containing 30 ml of deionized water and incubated at room temperature. At certain intervals, the swollen membranes were withdrawn from the water. The wet weight of the swollen membranes (W_{wet}) was measured after the removal of excess surface water by gently blotting with a filter paper. The swelling behavior and moisture content of the membranes were defined by the following equations: swelling ratio (%) = $(W_{wet} - W_{dry})/W_{dry} \times 100$ and moisture content ratio (%) = $(W_{wet} - W_{dry})/W_{wet} \times 100$. These tests were carried out at least in quadruplets ($n \geq 4$).

2.2.4. Water retention property

The water-conserved capacity of membranes was evaluated by the water retention test. After measuring the initial dry weight (W_{dry}), membranes were immersed in deionized water for 24 h. The swollen membranes were then wiped with a filter paper to remove surface water and placed in open mouth dishes at room temperature. After a specific period, the specimens were taken out and weighed (W_{wet}) again. The water retention ratio was defined by the following equation: water retention ratio (%) = $(W_{wet} - W_{dry})/W_{dry} \times 100$.

2.2.5. Water vapor transmission

The water vapor transmission (WVT) of the membranes was determined according to the ASTM E96 standard method. Briefly, each membrane specimen was used to seal the mouth of a cylindrical cup (2.75 cm in diameter) containing 30 ml of deionized water. The membrane was fastened tightly by barrier tapes to prevent any moisture loss. The membrane-cup assembly was placed in an incubator at an isothermal atmosphere of 37 °C. Evaporation of water through the membrane specimen was determined by periodic weightings. The weight changes indicated the loss of water. The profile of weight loss was plotted versus time for each sample. The water vapor transmission rate (WVTR) was calculated by dividing the daily weight loss of water with the area of cup opening. The measurement was repeated five times for each sample.

2.2.6. Mechanical test

The mechanical properties were determined by a universal testing machine (HT-8504 Hung Ta Instruments, Taiwan) in tensile mode. Each membrane was cut into dumbbell-shaped. The specimen was stretched at a crosshead speed of 100 mm/min to reach a constant strain rate. Young's modulus, tensile strength and percentage elongation at break were calculated from the stress-strain data (Akturk et al., 2011). Five specimens were measured to obtain the average values.

2.3. Cytotoxicity and cell attachment tests

Mouse skin fibroblast cells (L929) were purchased from the Bioresource Collection and Research Center and cultured in low-glucose Dulbecco's modified Eagle medium (DMEM) (Gibco, USA) containing 10% fetal bovine serum (FBS) (SAFC Biosciences, USA), 1% Antibiotic–Antimycotic solution (Caisson, USA), and 1.5 g/L sodium bicarbonate (Sigma, USA) in an incubator at 37 °C under 5% CO_2/95% air and 99% relative humidity. For the cytotoxicity evaluation, L929 fibroblasts were seeded in 24-well tissue culture plates with an initial density of 5×10^4 cells per well. After 24 h, the medium was replaced by fresh medium containing the BC extract. The extraction conditions were based on ISO 10993-12. Briefly, BC were extracted at 37 °C for 24 h in culture media at a 6 cm^2/ml extraction ratio. The culture medium was used as the negative control,

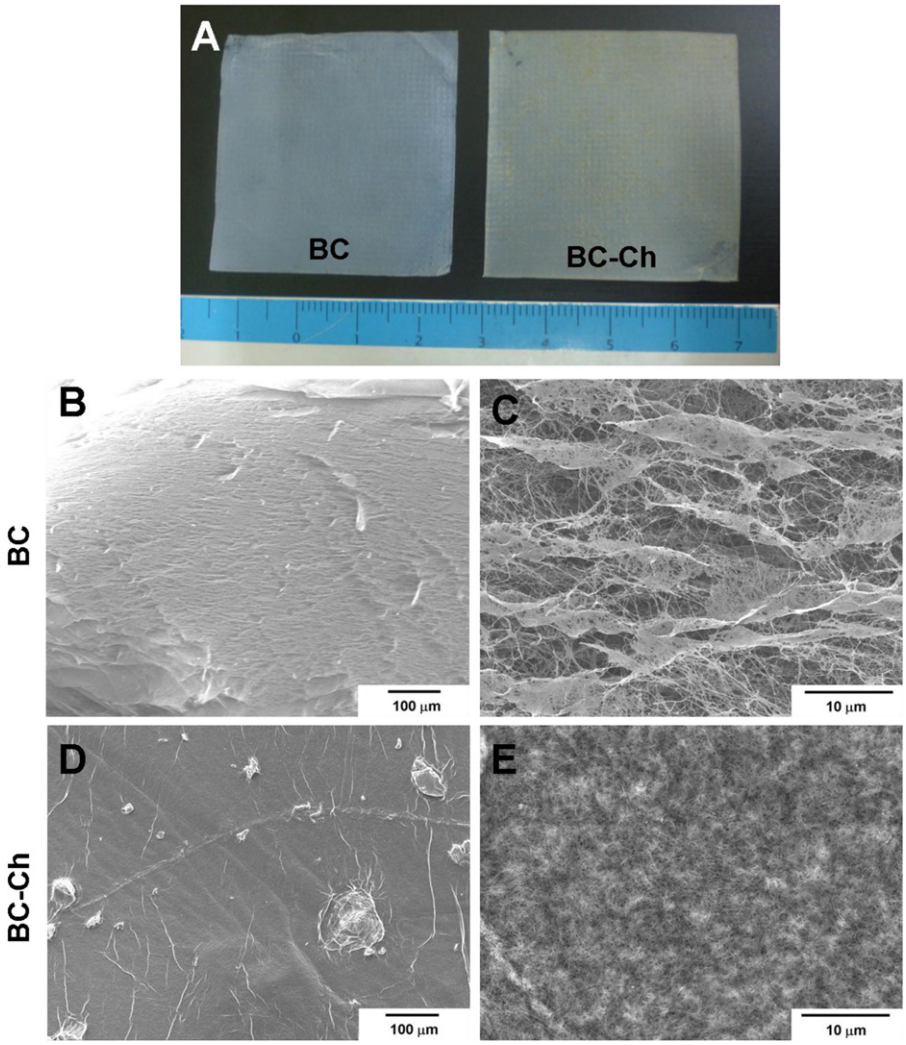

Fig. 1. (A) The gross appearance and (B–E) SEM images of BC and BC–Ch membranes. (B and C) were taken from the surface of BC membranes and (D and E) were taken from the surface of BC–Ch membranes. Magnification: (B and D) at 150× and (C and E) at 2500×.

while that containing 10% dimethyl sulfoxide (DMSO) (Sigma, USA) was used as the positive control. After incubation for 24 h, cell viability was measured by the 3-(4,5-dimethylthiazol-2-yl)-2,5-diphenyltetrazolium bromide (MTT) assay (Sigma, USA), where MTT was turn into purple formazan after reduction by mitochondrial enzymes in living cells. The formazan was dissolved in DMSO and the UV–vis absorbance at 550 nm was analyzed in a microplate reader (SpectraMax M5, Molecular Devices, USA). To evaluate the cell attachment on BC and BC–Ch membranes, the membranes were placed in 24-well tissue culture plates, where L929 fibroblasts were seeded in a density of 5×10^4 cells per well. A blank well (tissue culture polystyrene, TCPS) served as the control. After incubation for 24 h, the membranes were washed with PBS and the adherent cells were quantified by the MTT assay. For each group, three parallel samples were used in the cytotoxicity test, and six in the cell attachment study.

2.4. Antibacterial assessment

The antibacterial activity of BC and BC–Ch was analyzed according to the Japanese Industrial Standard JIS Z 2801:2000. The bacterial strains used for the experiment were *Escherichia coli* and *Staphylococcus aureus*, which were purchased from the Bioresource Collection and Research Center. Both of the bacteria were cultivated in nutrient broth containing 3 g beef extract (Himedia, India), 10 g peptone (Becton, Dickinson and Company (BD), USA), and 5 g sodium chloride (Sigma, USA) per 1000 ml water. The sample films were swollen and placed in petri dishes and inoculated with 400 μl of bacterial cell suspension (2.5×10^5 to 1×10^6 CFU/ml) at a temperature of 35 °C and a relative humidity of 90%. After an immediate contact (control) or 24 h of contact time, the residual bacteria were washed out and diluted serially for colony counting. Aliquots of diluted solution (100 μl) were spread on agar plates. After incubation at 37 °C for 24 h, colonies on the agar were counted visually and as CFU per sample. The bacterial growth inhibition was calculated by the following equation: antibacterial efficiency = $(N_0 - N)/N_0$, where N_0 and N each represents the bacteria number of control and experimental group. The measurement was repeated six times for each group.

2.5. Wound healing experiments

Wound healing experiments of BC and BC–Ch membranes were compared with the commercial Tegaderm™ hydrocolloid dressings and transparent film dressings, both of which were manufactured by 3 M Health Care Ltd. (USA). Eighteen 8-weeks-old male *Sprague Dawley* rats were obtained from BioLASCO Taiwan Co., Ltd. After hair removal and anesthesia, two to three 1.2 cm × 1.2 cm

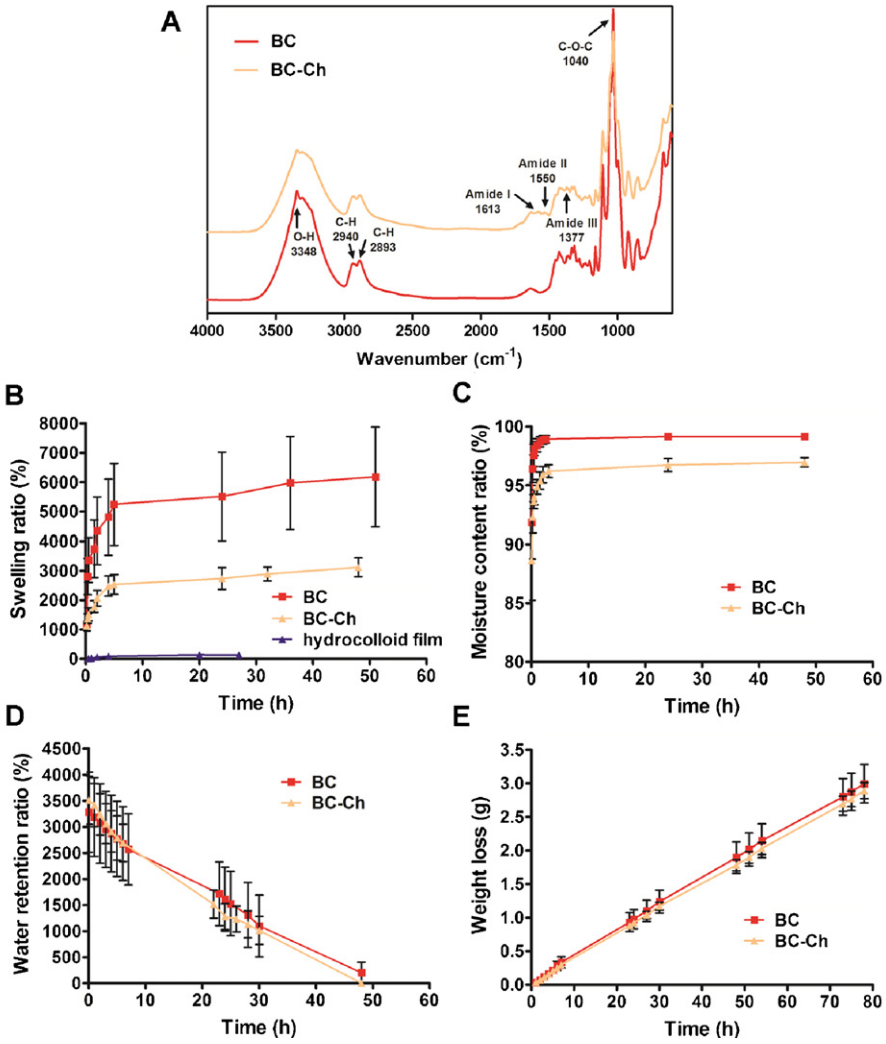

Fig. 2. Physico-chemical characteristics for BC and BC–Ch membranes: (A) FTIR spectra, (B) swelling ratio, (C) moisture content ratio, (D) water retention ratio, and (E) water vapor transmission profiles.

wounds were created on the dorsum of the rats. The defects were through the skin and panniculus carnosus. Animals were divided into two groups. In the first group, each wound was covered with a piece of BC, 3 M Tegaderm™ hydrocolloid dressing (abbreviated as "hydrocolloid film") or Tegaderm™ transparent film dressing (abbreviated as "transparent film"). In the second group, each wound was covered by a piece of BC or BC–Ch membrane. All membranes were sterilized by gamma irradiation (25 kGy). A self-adherent wrap (Coban™, 3 M Health Care) was employed to fix the dressings to the wounds. Dressings were changed to new ones every 2 or 3 days. The observation on wound closure was made at 1, 3, 6, 8, 10, 13, 15, 17, and 20 days for the first group, and at 1, 3, 5, 7, 10, 13, 15, 17, and 20 days for the second group. The wound size was determined by digital imaging and ImageJ software (National Institutes of Health, USA). The percentage of wound closure was calculated using the following formula: $(A_0 - A)/A_0 \times 100$ (%), where A_0 and A each represent the wound area at day 0 and at different observation points.

At 7 and 14 days, the rats were sacrificed and samples were obtained from the wound and the surrounding skin. The tissue specimens were fixed in a 4% formaldehyde solution for 24 h and embedded in paraffin. The specimens were sectioned into 5-μm thick slices in perpendicular to the surface of wound. The histological sections were stained with hematoxylin and eosin (H&E) reagent and examined under an optical microscope (Nikon Eclipse 80i, Japan).

3. Results and discussion

3.1. Characterization of BC and the composites

3.1.1. Morphology of BC and BC–Ch membranes

The surface morphology of the original BC membranes and BC–Ch composites as examined by SEM is shown in Fig. 1. A well-organized three-dimensional fibrillar network was observed for BC membranes (Fig. 1(B)). The matrix consists of randomly arranged fibrils and a variety of empty space in-between (Fig. 1(C)). Based on literature, the bacteria polymerize glucose molecules through β-(1→4) glucan chains, and excrete the polymer to the extracellular space to form nanofibrils that are further organized and stabilized by intramolecular hydrogen bonds to generate an ultrafine reticulated structure (Yano, Maeda, Nakajima, Hagiwara, & Sawaguchi, 2008). Our finding of BC membranes was consistent with that described in literature. BC–Ch membranes were even more compact probably due to the presence of chitosan on the surface (Fig. 1(D and E)). It has been reported that chitosan may penetrate into the pores of bacterial cellulose and interact with the microfibrils, which may affect the physico-chemical properties

(Cai & Yang, 2011; Ul-Islam, Shah, Ha, & Park, 2011). Our data suggested that chitosan may incorporate with the microfibrils of BC membranes, forming a denser network structure, and decreasing the pore size.

3.1.2. FTIR studies

FTIR spectra obtained from BC and BC–Ch membranes are shown in Fig. 2(A). For pure BC, a broad characteristic peak at 3348 cm^{-1} was assigned to O—H stretching vibration. The peaks at 2940 cm^{-1} and 2893 cm^{-1} were attributed to aliphatic C—H stretching vibration. Another intense peak located at 1040 cm^{-1} was ascribed to C—O—C stretching vibration. For BC–Ch membranes, the characteristic bands of BC remained to be present; moreover, some additional peaks appeared in the spectrum. These peaks including 1613 cm^{-1} (amide I), 1550 cm^{-1} (amide II), and 1377 cm^{-1} (amide III) came from the characteristic amide groups of chitosan. The FTIR spectra helped to verify the presence of chitosan molecules in BC–Ch membranes.

3.1.3. Water absorptivity, water retention property and water vapor transmission

A moist environment can promote the penetration of the active substances, protect wounds against bacterial invasion, and provide a painless removal from wound surface after recovery (Shezad, Khan, Khan, & Park, 2010). An ideal wound dressing should lock the exudate, as well as maintain proper wound moisture during the healing process. Therefore, measurements of the swelling behavior, moisture content, water retention capacity, and water vapor transmission rate of the BC dressings were performed. These data are presented in Fig. 2. Fig. 2(B and C) showed that the samples were almost saturated with water after being immersed in deionized water for 24 h. The swelling ratio of BC was about 60 times of its dry weight, and was much higher than that of the hydrocolloid films (Fig. 2(B)). The addition of chitosan, as in BC–Ch, decreased the swelling ratio to about half that of BC. The water absorption capacity of BC membranes was about 99% (Fig. 2(C)), while that of BC–Ch was about 97%. The difference in the water absorption capacity between BC and BC–Ch could be explained by their respective porous structure. Water molecules were thought to be physically trapped by the delicate network structure of bacterial cellulose (Ul-Islam, Khan, & Park, 2012). The incorporation of chitosan may make the surface more compact with smaller porosity, which reduced the water uptake. On the other hand, the water retention ratios evaluated over a period of 48 h showed no significant difference between BC and BC–Ch (Fig. 2(D)). The water evaporation rates were higher initially for both membranes, which was ascribed to the rapid escape of the surface water. The water retention ratio of BC–Ch remained nearly constant (except for the initial period). It took about 48 h for the complete evaporation of the adsorbed water. In addition to water retention, the water loss from open wounds is related to the water permission of the dressings. According to Fig. 2(E), the rate of water vapor permission was nearly constant for BC and BC–Ch membranes. The corresponding WVTR of BC was 1503 g/m^2/day and that of BC–Ch was 1460 g/m^2/day (data not shown), which had no statically significant difference between each other. The typical WVTR of normal skin is 204 g/m^2/day. The WVTR of injured skin varies in a broad range, from 279 g/m^2/day for a first-degree burn to 5138 g/m^2/day for a granulating wound (Wu et al., 2004). Overall, the results in Fig. 2 demonstrated that BC and BC–Ch could maintain a suitable moisture environment for low- to mid-range exudative wounds without excessive dehydration. This was believed to be associated with the microfibrils in both membranes that helped to retain water molecules efficiently through the strong hydrogen bonding interactions.

Table 1
Tensile properties of BC and BC–Ch membranes.

Materials	Young's modulus (MPa)	Tensile strength (MPa)	Elongation at break (100%)
BC	33.57 ± 4.13	14.77 ± 2.05	32.17 ± 2.85
BC–Ch	132.19 ± 45.87	10.26 ± 1.52	28.54 ± 7.76

3.1.4. Mechanical test

In addition to the moist environments, wound dressings should maintain the integrity during use. The mechanical properties of BC and BC–Ch membranes are presented in Table 1. For pure BC, the tensile strength was about 15 MPa and the elongation at break was about 32%. For BC–Ch membranes, the tensile strength was about 10 MPa and the elongation at break was about 29%. The Young's modulus obtained from the stress–strain curve was about 34 and 132 MPa for BC and BC–Ch membrane, respectively. The tensile strength of bacterial cellulose reported in a previous study was 100–260 MPa (Yano et al., 2008), which was higher than that of BC in this study. Nevertheless, the values may vary from different situations such as culture time, medium supplement, or post treatment (Cai & Yang, 2011). The higher Young's modulus of BC–Ch membrane was attributed to the addition of chitosan. The elongation at break (29–32%) for BC and BC–Ch membranes indicated

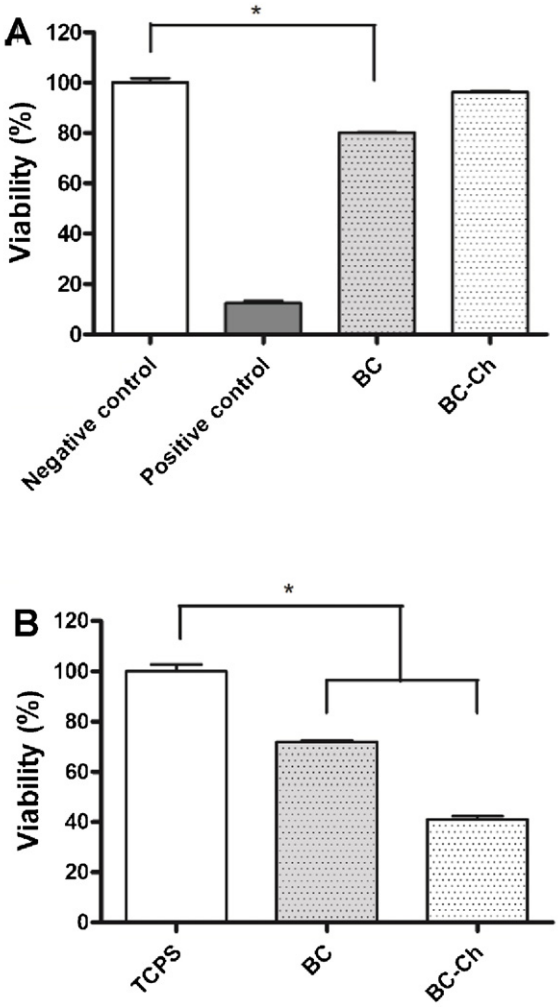

Fig. 3. Biocompatibility of BC and BC–Ch: (A) Cytotoxic effect of the extracts (L929 fibroblasts, 24 h incubation) and (B) cell attachment on materials (L929 fibroblasts, 24 h incubation).

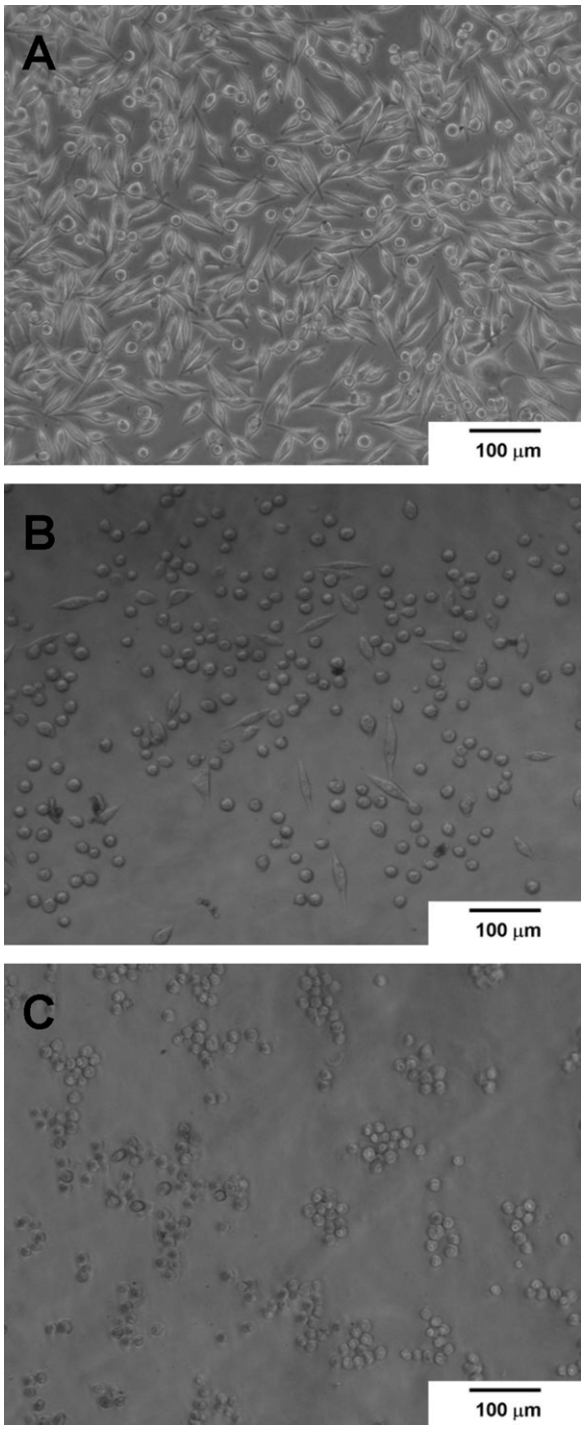

Fig. 4. Cell morphology of L929 fibroblasts on (A) TCPS: negative control, (B) BC, and (C) BC–Ch membranes for 24 h incubation.

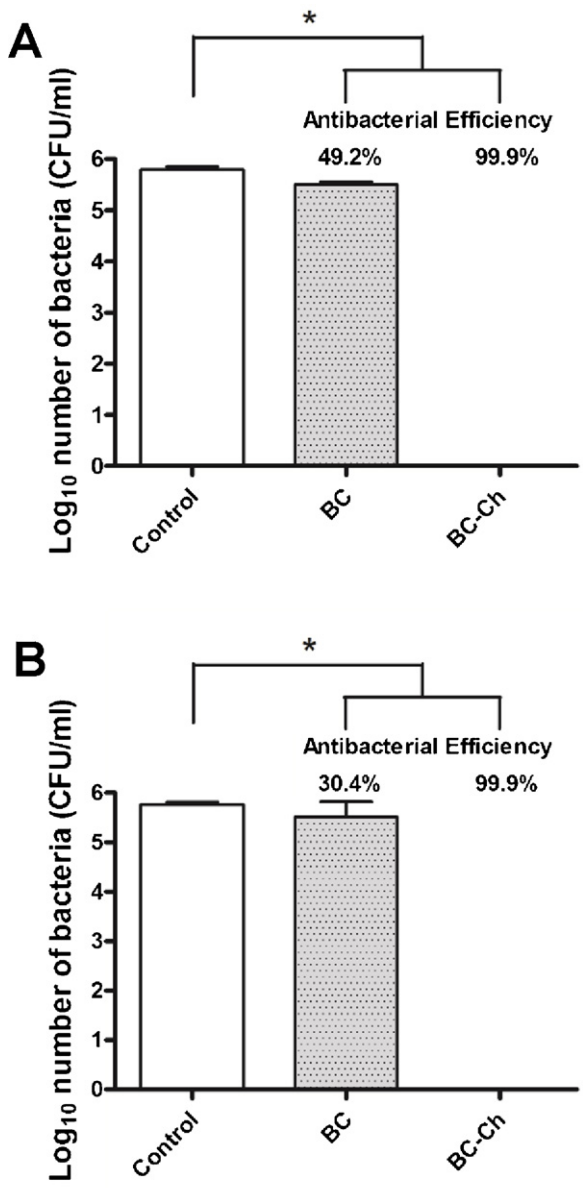

Fig. 5. Antibacterial activity of BC and BC–Ch membranes against (A) *E. coli* and (B) *S. aureus*.

adequate toughness, which allowed the dressings to fit well in the wound sites.

3.2. Cytotoxicity and cell attachment

The in vitro biological properties of BC and BC–Ch were examined by measuring the cytotoxicity and cell attachment through indirect and direct contact studies. Results from the cytotoxicity test of BC and BC–Ch extracts (i.e. indirect contact) on L929 fibroblasts are shown in Fig. 3(A). A slightly lower viability was observed for fibroblasts upon incubation with the extract of BC, which was consistent with the literature (Moreira et al., 2009). The lower viability may be related to the unknown component generated during the synthetic process of BC. Nevertheless, a 15% reduction is considered acceptable for wound dressing applications. On the other hand, the extract of BC–Ch membranes did not affect the viability of fibroblasts at all. There may be some other component in the BC–Ch extract that eliminated the slight negative effect of BC extract on cell viability.

The viability of L929 fibroblasts attached on the membranes (i.e. direct contact) is shown in Fig. 3(B). Here the viability reflected the extent of cell attachment. The number of cells on BC membranes was more than 70% vs. TCPS. On BC–Ch membranes, the number of attached cells decreased and was about 40% vs. TCPS. Fig. 4 shows the morphology of attached fibroblasts on BC and BC–Ch membranes. There were many cells attached on both materials. Some of the cells remained in round shape (not spread) during the experimental period, especially on BC–Ch membranes. Cell attachment involves multiple steps including the adsorption of binding proteins, recognition of extracellular matrix, and rearrangement

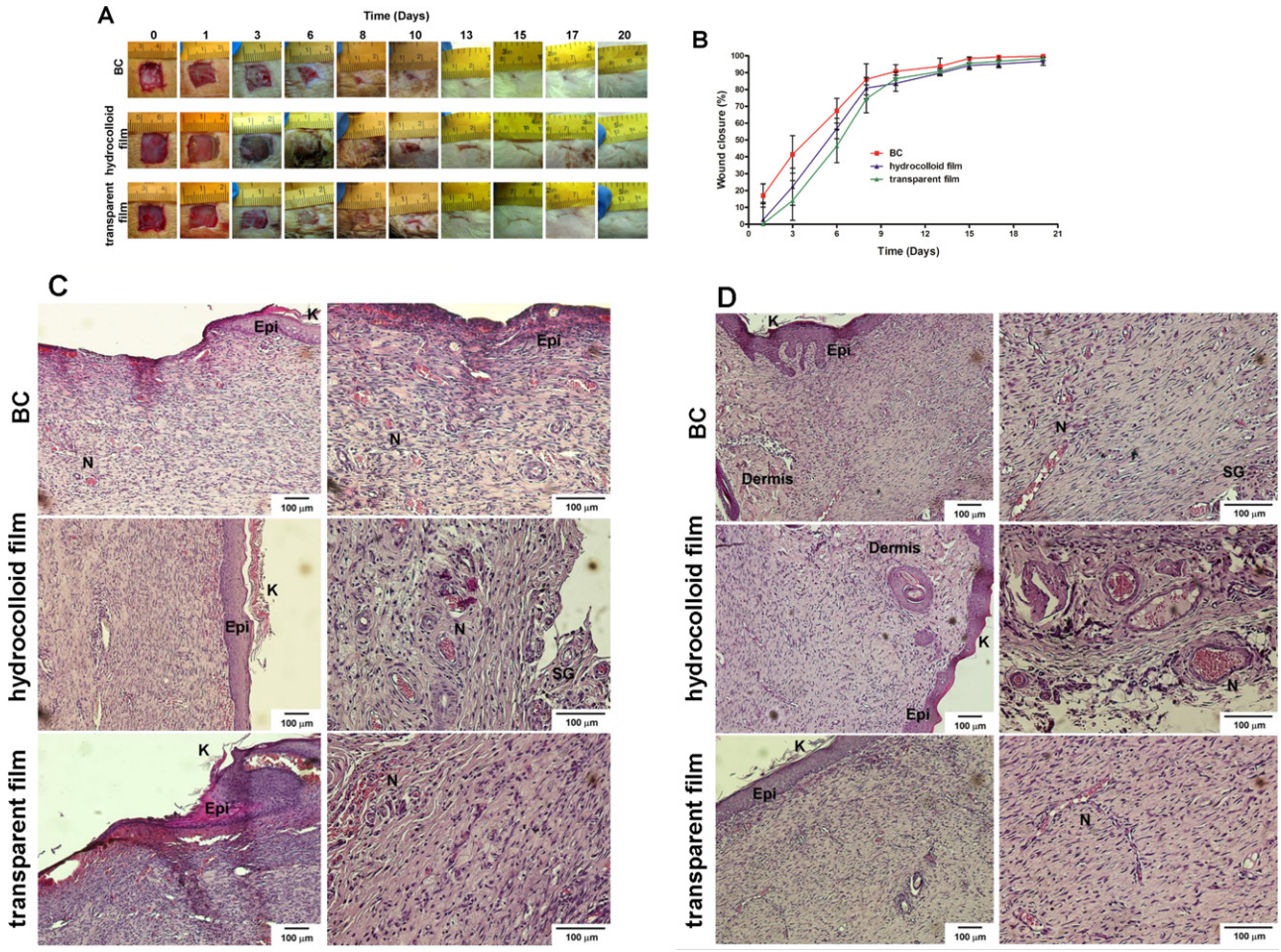

Fig. 6. Effects of BC on wound healing. Hydrocolloid and transparent films were commercial products and used for comparison. (A) Images of wounds in SD-rats. (B) Ratio of wound closure during wound healing ($n = 9$ at days 1, 3 and 6; $n = 6$ at days 8, 10 and 13; $n = 3$ at days 15, 17 and 20). (C and D) Histology of wounds treated with BC for 7 days (C) and 14 days (D). K: Keratin layer, Epi: Epidermis, N: Neovascularization, F: Hair follicles, SG: sebaceous glands.

of cytoskeleton (Pierschbacher & Ruoslahti, 1984; Ruoslahti & Pierschbacher, 1986). During the process, there may be other factors that affect the cell–material interaction. It was suggested that cell attachment on chitosan may depend on the environmental pH, molecular weight, and the percent of deacetylation (Chen, Chung, Wang, & Young, 2012; Hamilton et al., 2006; Mao et al., 2004). Further investigation is needed to clarify the significance of cell adhesion on BC and BC–Ch membranes.

3.3. Antibacterial assessment

Bacterial infection can seriously affect wound healing. Since chitosan is antibacterial, the incorporation of chitosan was expected to decrease the bacterial growth on BC. The antibacterial properties of BC and BC–Ch membranes were evaluated by direct contact with *E. coli* or *S. aureus* for 24 h. The numbers of colony of these bacteria were presented on a logarithm scale as shown in Fig. 5. It was noted that there was a 49.2% and 99.9% reduction in viable *E. coli* on BC and BC–Ch membranes, respectively (Fig. 5(A)). For *S. aureus*, a growth inhibition of 30.4% was observed on BC and 99.9% was observed on BC–Ch (Fig. 5(B)). BC–Ch demonstrated remarkable bacterial inhibition against Gram-negative *E. coli* and Gram-positive *S. aureus*. These results also revealed that the addition of chitosan in bacterial cellulose significantly increased the antibacterial efficiency. According to literature, the antibacterial activity of chitosan falls into two proposed mechanisms, both of which is related to the amount of active amino groups (Goy, de Britto, & Assis, 2009). In one mechanism, the positively charged chitosan would interact with the negatively charged bacteria surface, leading to an increase of bacterial membrane permeability and cell growth inhibition. The other mechanism is that binding of chitosan with DNA may suppress the mRNA generation of bacteria. In the case of BC membranes, the reduction in viable counts (49.2% for *E. coli* and 30.4% for *S. aureus*) may be ascribed to the rough surface where bacteria could not attach properly. In the disc diffusion method, no inhibition zone was observed for BC and BC–Ch membranes against *E. coli* and *S. aureus* (Fig. S1). This suggested that chitosan may be tightly incorporated in BC fibrils so the antibacterial component did not readily diffuse to the surrounding agar to create the inhibition zone.

Supplementary data associated with this article can be found, in the online version, at http://dx.doi.org/10.1016/j.carbpol.2013.01.076.

3.4. Wound healing experiments

BC and BC–Ch membranes were compared with the commercially available 3 M Tegaderm hydrocolloid and transparent films for their effects on skin wound healing in rat models. Fig. 6(A) presents the macroscopic appearance of wounds covered with BC, hydrocolloid films, or transparent films. BC membranes and hydrocolloid films could be removed from the wounds easily without causing any interference with the healing process. Stripping off 3 M transparent films, however, resulted in slight damage to the

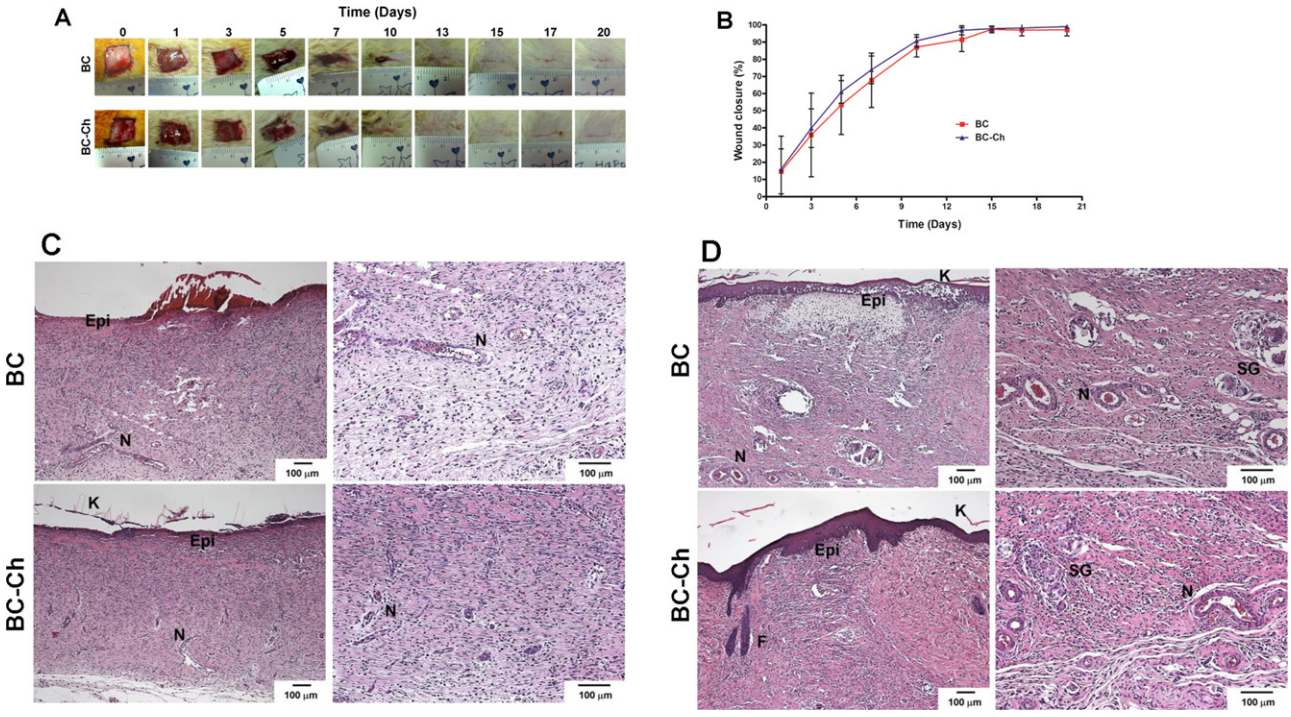

Fig. 7. Effects of BC–Ch on wound closure, compared with BC. (A) Images of wounds in SD-rats. (B) Ratio of wound closure during wound healing (n = 9 at days 1, 3, 5 and 7; n = 6 at days 10, 13 and 15; n = 3 at days 17 and 20). (C and D) Histology of wounds treated with BC–Ch for 7 days (C) and 14 days (D). K: Keratin layer, Epi: Epidermis, N: Neovascularization, F: Hair follicles, SG: sebaceous glands.

wounds, which prolonged the recovery. At the sixth day, epithelialization at the wound sites was observed. Wounds treated with BC membranes contracted faster than the other groups. Neither scab nor inflammation was observed in each group during the healing process. The closure rates of wounds were quantified and are shown in Fig. 6(B). Apparently, the wounds treated with BC membranes healed more rapidly, as compared with those treated with hydrocolloid or transparent films. BC showed 85% closure in average after 8 days. At the thirteenth day, BC treated wounds were almost healed.

Histological examinations for wounds in different groups are shown in Fig. 6(C and D). At day 7, the granulation tissue in the dermis was observed in each group (Fig. 6(C)). In addition, the epithelialization process was activated at the surface of the wounds. BC-treated wounds were nearly covered by a thin layer of superficial neoepithelium. The granulation tissue comprised abundant fibroblasts as well as capillaries in wounds treated with BC membranes. For the hydrocolloid group, wounds were nearly re-epithelialized too, accompanied by an integral layer of keratin. Neovascularization was also observed in the hydrocolloid group. Some skin appendages such as sebaceous glands could be seen in the wound area. The transparent film-treated wounds possessed the lowest epithelialization rate, compared with the others. Neoepithelium was only discernible at the margin. At day 14, all wounds were covered with a layer of epidermis with mature stratum corneum (Fig. 6(D)). The dermis showed an increased deposition of organized collagen fibers. These results indicated that the healing process was in the late epidermal proliferative phase. For BC and the hydrocolloid group, the thickness of epidermis was close to that of normal skin. It was also found that the epidermal basement layer in BC-treated wounds connected more tightly to the dermis. The latter result may be ascribed to the abundance of type IV collagen, which plays an important role in strengthening and stabilizing the skin (Pöschl et al., 2004). Wounds treated with BC membranes showed better tissue regeneration, in comparison with those treated with commercial hydrocolloid or transparent films.

The macroscopic observation for wounds treated with BC and BC–Ch membranes is illustrated in Fig. 7(A). In the first 3 days, there was a large amount of fluid accumulated in the wounds. With well-organized network structure, these two membranes exhibited effective exudation absorption capacity for wounds. The replacement of wound dressings did not cause damage to the regenerated wounds, as the membranes could be easily detached from the wound surface. During the third to tenth day, the new epidermis rapidly grew at the wound sites, from the margin to the center, and wounds were contracted. The wound closure rates for BC and BC–Ch membranes-treated wounds are displayed in Fig. 7(B). Although there was no significant difference in wound closure between the two groups, the average contraction ratio in the BC–Ch group was always greater than that in the BC group at each time interval. The results also indicated that BC–Ch was more efficient in wound contraction, which may be attributed to the chitosan component in BC–Ch (Ueno et al., 1999).

The effect of BC and BC–Ch membranes on wound healing was further evaluated by histology (Fig. 7(C and D)). At day 7, an organized layer of superficial neoepithelium had covered the wound surface, and neovascularization was observed at the wound sites. Keratin formation in BC–Ch-treated wounds was more integrated (Fig. 7(C)). At day 14, the extents of epithelialization and capillary formation obviously increased in BC-treated wounds (Fig. 7(D)). Some sebaceous glands could also be observed. For the BC–Ch group, the repaired dermis was similar in morphology to normal skin. The multilayered epidermis and stratum corneum were fully integrated and discernible. Furthermore, the newly developed hair follicles could be seen in the wound areas. The epidermis and dermis were anchored tightly in BC–Ch-treated wounds, which as mentioned may correlate to the generation of type IV collagen. Skin wound healing is a complex process which involves four major phases including hemostasis, inflammation,

proliferation, and remodeling (Diegelmann & Evans, 2004). It is generally considered that wounds reepithelialize more rapidly in a moist environment (Chiu, Lee, Chu, Chang, & Wang, 2008). BC and its composite with chitosan have good water absorption capacity and optimal water permeability, which offers proper conditions to facilitate wound healing. In addition, these membranes fit the wound very well while can be easily removed without secondary injury. The incorporation of chitosan in BC further accelerates the healing process. Taken together, these results suggest the potential usage of BC–Ch membranes as wound dressings.

4. Conclusions

BC and BC–Ch membranes were successfully prepared in this study. SEM images showed that BC had a well-organized three dimensional fibrillar network with plenty of pore spaces. The incorporation of chitosan in BC (i.e. BC–Ch) led to a more compact network with smaller pore size. Results from the water swelling, moisture content, water retention, and permeability tests showed that BC and BC–Ch membranes had balanced functionality of water absorption and dehydration that helped maintain at suitable moisture content for wound healing applications. These membranes had proper mechanical properties and cytocompatibility. Especially, the antibacterial evaluation revealed that the addition of chitosan into BC significantly increased the growth inhibition against *E. coli* and *S. aureus*. Animal studies showed that wounds covered with BC–Ch healed more rapidly than wounds covered with BC, as well as those covered with commercial Tegaderm hydrocolloid or transparent films. The epithelialization and regeneration process proceeded faster in the BC–Ch-covered wounds than the other groups based on histology. These results demonstrated the good potential of BC–Ch membranes in wound treatment.

Acknowledgment

This research was sponsored by the National Science Council (NSC 98-2622-E-002-018-CC2 and NSC 99-2622-E-002-021-CC2).

References

Akturk, O., Tezcaner, A., Bilgili, H., Deveci, M. S., Gecit, M. R., & Keskin, D. (2011). Evaluation of sericin/collagen membranes as prospective wound dressing biomaterial. *Journal of Bioscience and Bioengineering*, *112*(3), 279–288.

Alvarez, O. M., Patel, M., Booker, J., & Markowitz, L. (2004). Effectiveness of a biocellulose wound dressing for the treatment of chronic venous leg ulcers: Results of a single center randomized study involving 24 patients. *Wounds*, *16*(7), 224–233.

Bäckdahl, H., Helenius, G., Bodin, A., Nannmark, U., Johansson, B. R., Risberg, B., et al. (2006). Mechanical properties of bacterial cellulose and interactions with smooth muscle cells. *Biomaterials*, *27*(9), 2141–2149.

Cai, Z., Hou, C., & Yang, G. (2011). Preparation and characterization of a bacterial cellulose/chitosan composite for potential biomedical application. *Journal of Applied Polymer Science*, *121*(3), 1488–1494.

Cai, Z., Hou, C., & Yang, G. (2012). Poly(3-hydroxubutyrate-co-4-hydroxubutyrate)/bacterial cellulose composite porous scaffold: Preparation, characterization and biocompatibility evaluation. *Carbohydrate Polymers*, *87*(2), 1073–1080.

Cai, Z., & Yang, G. (2011). Bacterial cellulose/collagen composite: Characterization and first evaluation of cytocompatibility. *Journal of Applied Polymer Science*, *120*(5), 2938–2944.

Chen, Y. H., Chung, Y. C., Wang, I. J., & Young, T. H. (2012). Control of cell attachment on pH-responsive chitosan surface by precise adjustment of medium pH. *Biomaterials*, *33*(5), 1336–1342.

Chiu, C. T., Lee, J. S., Chu, C. S., Chang, Y. P., & Wang, Y. J. (2008). Development of two alginate-based wound dressings. *Journal of Materials Science: Materials in Medicine*, *19*(6), 2503–2513.

Czaja, W., Krystynowicz, A., Bielecki, S., & Brown, R. M., Jr. (2006). Microbial cellulose – The natural power to heal wounds. *Biomaterials*, *27*(2), 145–151.

Diegelmann, R. F., & Evans, M. C. (2004). Wound healing: An overview of acute, fibrotic and delayed healing. *Frontiers in Bioscience*, *9*, 283–289.

Eichhorn, S. J., Baillie, C. A., Zafeiropoulos, N., Mwaikambo, L. Y., Ansell, M. P., Dufresne, A., et al. (2001). Review: Current international research into cellulosic fibres and composites. *Journal of Materials Science*, *36*(9), 2107–2131.

Goy, R. C., de Britto, D., & Assis, O. B. G. (2009). A review of the antimicrobial activity of chitosan. *Polimeros*, *19*, 241–247.

Hamilton, V., Yuan, Y., Rigney, D. A., Puckett, A. D., Ong, J. L., Yang, Y., et al. (2006). Characterization of chitosan films and effects on fibroblast cell attachment and proliferation. *Journal of Materials Science: Materials in Medicine*, *17*(12), 1373–1381.

Keshk, S., & Sameshima, K. (2006). Influence of lignosulfonate on crystal structure and productivity of bacterial cellulose in a static culture. *Enzyme and Microbial Technology*, *40*(1), 4–8.

Klemm, D., Schumann, D., Udhardt, U., & Marsch, S. (2001). Bacterial synthesized cellulose – Artificial blood vessels for microsurgery. *Progress in Polymer Science*, *26*(9), 1561–1603.

Kurosumi, A., Sasaki, C., Yamashita, Y., & Nakamura, Y. (2009). Utilization of various fruit juices as carbon source for production of bacterial cellulose by *Acetobacter xylinum* NBRC 13693. *Carbohydrate Polymers*, *76*(2), 333–335.

Legeza, V. I., Galenko-Yaroshevskii, V. P., Zinov'ev, E. V., Paramonov, B. A., Kreichman, G. S., Turkovskii, I. I., et al. (2004). Effects of new wound dressings on healing of thermal burns of the skin in acute radiation disease. *Bulletin of Experimental Biology and Medicine*, *138*(3), 311–315.

Li, Y., Chen, X. G., Liu, N., Liu, C. S., Liu, C. G., Meng, X. H., et al. (2007). Physicochemical characterization and antibacterial property of chitosan acetates. *Carbohydrate Polymers*, *67*(2), 227–232.

Li, H., Yang, J., Hu, X., Liang, J., Fan, Y., & Zhang, X. (2011). Superabsorbent polysaccharide hydrogels based on pullulan derivate as antibacterial release wound dressing. *Journal of Biomedical Materials Research*, *98*(1), 31–39.

Maneerung, T., Tokura, S., & Rujiravanit, R. (2008). Impregnation of silver nanoparticles into bacterial cellulose for antimicrobial wound dressing. *Carbohydrate Polymers*, *72*(1), 43–51.

Mao, J. S., Cui, Y. L., Wang, X. H., Sun, Y., Yin, Y. J., Zhao, H. M., et al. (2004). A preliminary study on chitosan and gelatin polyelectrolyte complex cytocompatibility by cell cycle and apoptosis analysis. *Biomaterials*, *25*(18), 3973–3981.

Moreira, S., Silva, N. B., Almeida-Lima, J., Rocha, H. A., Medeiros, S. R., Alves, C., Jr., et al. (2009). BC nanofibres: In vitro study of genotoxicity and cell proliferation. *Toxicology Letters*, *189*(3), 235–241.

Nishi, Y., Uryu, M., Yamanaka, S., Watanabe, K., Kitamura, N., Iguchi, M., et al. (1990). The structure and mechanical properties of sheets prepared from bacterial cellulose. Part 2: Improvement of the mechanical properties of sheets and their applicability to diaphragms of electroacoustic transducers. *Journal of Materials Science*, *25*, 2997–3001.

Pierschbacher, M. D., & Ruoslahti, E. (1984). Cell attachment activity of fibronectin can be duplicated by small synthetic fragments of the molecule. *Nature*, *309*(5963), 30–33.

Pillai, C. K. S., Paul, W., & Sharma, C. P. (2009). Chitin and chitosan polymers: Chemistry, solubility and fiber formation. *Progress in Polymer Science*, *34*(7), 641–678.

Phisalaphong, M., & Jatupaiboon, N. (2008). Biosynthesis and characterization of bacteria cellulose–chitosan film. *Carbohydrate Polymers*, *74*, 482–488.

Pöschl, E., Schlötzer-Schrehardt, U., Brachvogel, B., Saito, K., Ninomiya, Y., & Mayer, U. (2004). Collagen IV is essential for basement membrane stability but dispensable for initiation of its assembly during early development. *Development*, *131*(7), 1619–1628.

Rabea, E. I., Badawy, M. E., Stevens, C. V., Smagghe, G., & Steurbaut, W. (2003). Chitosan as antimicrobial agent: Applications and mode of action. *Biomacromolecules*, *4*(6), 1457–1465.

Rinaudo, M. (2006). Chitin and chitosan: Properties and applications. *Progress in Polymer Science*, *31*(7), 603–632.

Ruoslahti, E., & Pierschbacher, M. D. (1986). Arg-Gly-Asp – A versatile cell recognition signal. *Cell*, *44*(4), 517–518.

Shah, J., & Brown, R. M., Jr. (2005). Towards electronic paper displays made from microbial cellulose. *Applied Microbiology and Biotechnology*, *66*(4), 352–355.

Shezad, O., Khan, S., Khan, T., & Park, J. K. (2010). Physicochemical and mechanical characterization of bacterial cellulose produced with an excellent productivity in static conditions using a simple fed-batch cultivation strategy. *Carbohydrate Polymers*, *82*(1), 173–180.

Takai, M. (1994). Bacterial cellulose. In R. D. Gilbert (Ed.), *Cellulose polymers, blends and composites* (pp. 233–240). Munich: Hanser.

Ueno, H., Yamada, H., Tanaka, I., Kaba, N., Matsuura, M., Okumura, M., et al. (1999). Accelerating effects of chitosan for healing at early phase of experimental open wound in dogs. *Biomaterials*, *20*(15), 1407–1414.

Ul-Islam, M., Khan, T., & Park, J. K. (2012). Water holding and release properties of bacterial cellulose obtained by in situ and ex situ modification. *Carbohydrate Polymers*, *88*(2), 596–603.

Ul-Islam, M., Shah, N., Ha, J. H., & Park, J. K. (2011). Effect of chitosan penetration on physico-chemical and mechanical properties of bacterial cellulose. *Korean Journal of Chemical Engineering*, *28*, 1736–1743.

Wu, Y. B., Yu, S. H., Mi, F. L., Wu, C. W., Shyu, S. S., Peng, C. K., et al. (2004). Preparation and characterization on mechanical and antibacterial properties of chitosan/cellulose blends. *Carbohydrate Polymers*, *57*(4), 435–440.

Yano, S., Maeda, H., Nakajima, M., Hagiwara, T., & Sawaguchi, T. (2008). Preparation and mechanical properties of bacterial cellulose nanocomposites loaded with silica nanoparticles. *Cellulose*, *15*, 111–120.

Yu, C. M., & Lien, C. C. (2012). Taiwanese patent pending (application no. 100145786) and Chinese patent pending (application no. 201110434084.6).